An adaptive Particle-In-Cell method using multi-resolution analysis

J.-P. Chehab[1], *A. Cohen, D. Jennequin, J. J. Nieto, Ch. Roland*[1] *and J. R. Roche*

[1]*Laboratoire de Mathématiques Paul Painlevé, UMR 8524*
Université de Lille 1, 59 655 Villeneuve d'Ascq Cédex, France
email: chehab@math.univ-lille1.fr, roland@math.univ-lille1.fr

Laboratoire Jacques-Louis Lions, Université Paris VI
Boîte courrier 187 75252 Paris Cedex 05 France
email: cohen@ann.jussieu.fr

Laboratoire J. Liouville, Centre Universitaire de la Mi-Voix
Maison de la Recherche Blaise Pascal, 50 rue F. Buisson, B.P. 699
62228 Calais Cedex France
email: jennequin@lmpa.univ-littoral.fr

Universidad de Granada, Facultad de Ciencias
Campus Universitario de Fuentenueva
Avda. Fuentenueva s/n 18071 Granada, Spain
email: jjmnieto@ugr.es

Institut de Mathématiques Élie Cartan, Université de Nancy I
B.P. 239, 54506 Vandoeuvre-lès-Nancy CedexFrance
email: roche@iecn.u-nancy.fr

Abstract. In this paper, we introduce a new PIC method based on an adaptive multi-resolution scheme for solving the one dimensional Vlasov–Poisson equation. Our approach is based on a description of the solution by particles of unit weight and on a reconstruction of the density at each time step of the numerical scheme by an adaptive wavelet technique: the density is firstly estimated in a proper wavelet basis as a distribution function from the current empirical data and then "de-noised" by a thresholding procedure. The so-called Landau damping problem is considered for validating our method. The numerical results agree with those obtained by the classical PIC scheme, suggesting that this multi-resolution procedure could be extended with success to plasma dynamics in higher dimensions.

1 Introduction

The kinetic motion of a physic plasma of charged particles in which the collisions between particles are neglected is usually modeled by the Vlasov equation [4],

$$\frac{\partial f}{\partial t} + v \cdot \nabla_x f - (E \cdot \nabla_v) f = 0, \quad (x, v) \in \mathbb{R}^d \times \mathbb{R}^d, \tag{1.1}$$

$f(x, v, t)$ being the distribution function and E the electrostatic field. The self-consistent field produced by the charge of the particles is

$$E_{\text{self}}(x, t) = -\nabla_x \phi_{\text{self}}(x, t), \tag{1.2}$$

where

$$-\Delta_x \phi_{\text{self}} = \rho(x, t), \quad \rho(x, t) = \int f(x, v, t)\, dv. \tag{1.3}$$

The system is closed with an initial data $f(x, v, 0) = f_0(x, v)$ and some decay conditions for the Poisson equation.

If $E = E_{\text{self}}$, this model is clearly dispersive due to the repulsive forces and then, in order to confine the particles in a bounded domain, as usual, we consider an additional given external potential $\phi_{\text{ext}}(x)$ and rewrite E as:

$$E(x, t) = E_{\text{self}} + E_{\text{ext}} := -(\nabla_x \phi_{\text{self}} + \nabla_x \phi_{\text{ext}}). \tag{1.4}$$

In this project we are interested in the numerical resolution of the repulsive VP system (1.1)–(1.2)–(1.4) endowed with an appropriate initial data by means of the *Particle-In-Cell* (PIC) method. In the classical PIC method (see [6], [12]) the initial data is approximated by a set of particles, and the method aims to follow the trajectories (the characteristic curves) of these particles. In order to reflect the distribution function f_0, the initial set of particles can either be uniformly distributed and weighted with the value of f_0 at the corresponding point, or distributed randomly according to the distribution function f_0 and identically weighted. In this paper we follow the second approach.

The main difficulty in the PIC method lies in the construction of the characteristic curves

$$\begin{cases} \dfrac{dX(t)}{dt} = V(t), \\ \dfrac{dV(t)}{dt} = E(X(t), t), \end{cases}$$

because of the nonlinearity due to the self-consistent potential. This requires to rebuild the charge density ρ at each time step in order to solve the Poisson equation and to obtain the electric field. Generally, this method gives good results with a relatively small number of particles but produces some numerical noise which prevent from describing precisely the tail of the distribution function. To overcome this drawback, it has been proposed to solve the problem by Eulerian methods [1] or semi Lagrangian methods [2]. Here, we propose to combine the PIC method with density estimation techniques based on wavelet thresholding [8] in order to reduce the noise level: the density $\rho(x, t)$ is estimated at time $t > 0$ by an expansion of the type

$$\sum_k \hat{c}_{J_1,k}\, \varphi_{J_1,k}(x) + \sum_{j=J_1}^{J_0} \Big(\sum_{k=0}^{2^j-1} T_\eta(\hat{d}_{j,k})\, \psi_{j,k}(x) \Big). \tag{1.5}$$

Here $\varphi_{J_1,k}$ and $\psi_{j,k}$ are the scaling functions and the wavelets, respectively. The scaling and detail coefficients $\hat{c}_{J_1,k}$ and $\hat{d}_{j,k}$ are estimated from the particle distribution at time t, and T_η is a thresholding operator at level η. Both the threshold level η and the finest resolution level J_0 are chosen depending on the number of particles.

The paper is organized as follows: in Section 2 we describe how the density is estimated by wavelets, in particular we present several thresholding strategies. Then, in Section 3 we present the new numerical scheme, making a comparison with the classical PIC method. In Section 4, we give a numerical illustration with the simulation of the so-called Landau damping.

2 Density estimation by wavelet thresholding

Wavelet decompositions have been widely studied since the last two decades both from the theoretical and practical point of view. In a nutshell, these decompositions are based on a hierarchy of nested approximation spaces $(V_j)_{j\geq 0}$ which should be thought as finite element spaces of mesh size $h \sim 2^{-j}$, endowed with a nodal basis of the form $\varphi_{j,k} := 2^{j/2}\varphi(2^j \cdot -k)$. The functions $\varphi_{j,k}$ are often referred to as primal scaling functions. A projector onto V_j is of the form

$$P_j f := \sum_k c_{j,k}\varphi_{j,k} \quad \text{with } c_{j,k} := \langle f, \tilde{\varphi}_{j,k}\rangle, \tag{2.1}$$

where $\tilde{\varphi}_{j,k}$ are dual scaling functions. The primal and dual wavelets $\psi_{j,k}$ and $\tilde{\psi}_{j,k}$ characterize the update between two successive level of approximation in the sense that

$$P_{j+1} f - P_j f := \sum_k d_{j,k}\psi_{j,k} \quad \text{with } d_{j,k} := \langle f, \tilde{\psi}_{j,k}\rangle, \tag{2.2}$$

We refer to [7] for a classical introduction on wavelets, [5] for more information on their application to numerical simulation of PDE's.

In the particular context of PIC methods, we are interested in the reconstruction of the density $\rho(x,t)$ from the locations $(x_i)_{i=1,\dots,N}$ of the particles at time t. As explained in the introduction, this reconstruction has the form (1.5) where $\hat{c}_{J_1,k}$ and $\hat{d}_{j,k}$ are estimators of the exact coefficients $c_{J_1,k} := \int \rho(x,t)\tilde{\varphi}_{J_1,k}(x)\,dx$ and $d_{J_1,k} := \int \rho(x,t)\tilde{\psi}_{j,k}(x)\,dx$ from the empirical distribution according to

$$\hat{c}_{J_1,k} := \frac{1}{N}\sum_{i=1}^{N} \varphi_{J_1,k}(x_i), \tag{2.3}$$

and

$$\hat{d}_{j,k} := \frac{1}{N} \sum_{i=1}^{N} \psi_{j,k}(x_i). \tag{2.4}$$

The interest of the thresholding procedure, in contrast to a simple projection or regularization at a fixed scale j which would compute $\sum_k \hat{c}_{j,k}\varphi_{j,k}$ is twofold: (i) the regularization level j is allowed to vary locally in the sense that the procedure might retain coefficients $d_{j,k}$ at scale j only for some k which typically corresponds to the regions where the density has sharp transitions and requires more resolution, and (ii) the local regularization level automatically adapts to the unknown amount of smoothness of the density through the thresholding procedure which only depends on the number N of samples.

Following Donoho *et al.* [8], the maximal scale level J_0 and the threshold η depend on the number of samples according to

$$2^{J_0} \sim N^{1/2} \tag{2.5}$$

and

$$\eta \sim \sqrt{\log(N)/N}. \tag{2.6}$$

Another choice proposed in [8] is a threshold parameter which also depends on the scale level j according to $\eta = \eta_j = K\sqrt{j/N}$. Two techniques are generally used to threshold the details: "hard" thresholding defined by $T_\eta(y) = y\chi_{\{|y|\geq\eta\}}$ and "soft" thresholding defined by $T_\eta(y) = \mathrm{Sign}(y)\max\{0, |y| - \eta\}$. We shall precise thresholding strategies that we choose for our applications in Section 4.

The density reconstruction method varies with the choice of the wavelet basis. This choice is dictated by two constraints:

1. Numerical simplicity: according to (2.3) and (2.4), the coefficients are estimated through the evaluation of dual scaling functions $\tilde{\varphi}_{J_1,k}$ and dual wavelets $\tilde{\psi}_{j,k}$ at the points x_i. It is therefore useful that these functions have a simple analytical form. In particular, high order compactly supported orthonormal wavelets cannot be used since they do not have an explicit analytical expression.

2. High order accuracy and smoothness: the primal wavelet system should have high order accuracy and smoothness in order to ensure the quality of the approximation of $\rho(x, t)$ by the expansion (1.5).

The choice of the Haar system is good with respect to the first constraint, since in this case the scaling function $\tilde{\varphi} = \varphi$ is simply the box function $\chi_{[0,1]}$, so that the estimation of a scaling coefficient $c_{j,k} = \langle \rho, \tilde{\varphi}_{j,k} \rangle$ simply amounts in counting the points falling in the interval $I_{j,k} = [2^{-j}k, 2^{-j}(k+1)[$:

$$\hat{c}_{j,k} := 2^{j/2} \frac{1}{N} \#\{i;\ x_i \in I_{j,k}\}. \tag{2.7}$$

In particular, we can compute the $\hat{c}_{J_0,k}$ at the finest scale level and use the Haar transform algorithm to compute the $\hat{d}_{j,k}$ according to the classical relations:

$$\hat{c}_{j,k} = \frac{\hat{c}_{j+1,2k} + \hat{c}_{j+1,2k+1}}{\sqrt{2}} \quad \text{and} \quad \hat{d}_{j,k} = \frac{\hat{c}_{j+1,2k} - \hat{c}_{j+1,2k+1}}{\sqrt{2}}. \tag{2.8}$$

However, this choice is not good with respect to the second constraint since piecewise constant functions are low order accurate. In order to fix this defect, while preserving the numerical simplicity of the method, we propose to use a higher order (third order) reconstruction still based on the box function $\chi_{[0,1]}$ as $\tilde{\varphi}$, as proposed by Ami Harten in [11]. This means that the coefficients $\hat{c}_{j,k}$ are still defined by (2.7), but the relation between the approximation and detail coefficients $\hat{c}_{j,k}$ and $\hat{d}_{j,k}$ is modified according to

$$\hat{d}_{j,k} = \frac{1}{\sqrt{2}}\hat{c}_{j+1,2k} - \hat{c}_{j,k} - \frac{1}{8}(\hat{c}_{j,k-1} - \hat{c}_{j,k+1}). \tag{2.9}$$

This is an instance of the so-called *lifting scheme* introduced in [14]. Using this relation, we estimate all the coefficients $c_{j,k}$ and $d_{j,k}$ for $J = J_1, \ldots, J_0 - 1$ and we apply the thresholding operator T_η to the estimated coefficients $\hat{d}_{j,k}$.

It should be remarked that the primal scaling functions $\varphi_{J_1,k}$ and wavelets $\psi_{j,k}$ do not have an explicit analytical expression, in contrast to the dual scaling functions and wavelets. However, we can reconstruct the estimator (1.5) at arbitrarily fine resolution by applying the reconstruction formulae

$$\hat{c}_{j+1,2k} = \sqrt{2}\Big[\hat{c}_{j,k} - \frac{1}{8}(\hat{c}_{j,k-1} - \hat{c}_{j,k+1}) + T_\eta(\hat{d}_{j,k})\Big], \tag{2.10}$$

and

$$\hat{c}_{j+1,2k+1} = \sqrt{2}\hat{c}_{j,k} - \hat{c}_{j+1,2k}. \tag{2.11}$$

It is also possible to construct wavelet-like multiscale decompositions where both the dual and primal functions have a simple analytical expression, based on the quasi-interpolation operator

$$P_j f := \sum_k c_{j,k}\varphi_{j,k}, \quad c_{j,k} = \langle f, \varphi_{j,k}\rangle, \tag{2.12}$$

where $\varphi = (1 - |x|)_+$ is the classical hat function. We therefore estimate the coefficients by

$$\hat{c}_{j,k} := \frac{1}{N}\sum_{i=1}^{N} \varphi_{j,k}(X_i), \tag{2.13}$$

at the finest scale $j = J_0$ and derive them recursively at coarser levels by the formula

$$\hat{c}_{j,k} = \frac{1}{\sqrt{2}}\hat{c}_{j+1,2k} + \frac{1}{2\sqrt{2}}(\hat{c}_{j+1,2k+1} + \hat{c}_{j+1,2k-1}).$$

In this case, the detail components at level j reads

$$(P_{j+1} - P_j)f = \sum_k [\hat{d}^0_{j,k}\varphi_{j+1,2k} + \hat{d}^+_{j,k}\varphi_{j+1,2k+1} + \hat{d}^-_{j,k}\varphi_{j+1,2k-1}], \tag{2.14}$$

with

$$\begin{aligned}
\hat{d}^0_{j,k} &:= \frac{\sqrt{2}-1}{\sqrt{2}}\hat{c}_{j+1,2k} - \frac{1}{2\sqrt{2}}\hat{c}_{j+1,2k+1} - \frac{1}{2\sqrt{2}}\hat{c}_{j+1,2k-1},\\
\hat{d}^+_{j,k} &:= \frac{2\sqrt{2}-1}{4\sqrt{2}}\hat{c}_{j+1,2k+1} - \frac{1}{2\sqrt{2}}\hat{c}_{j+1,2k} - \frac{1}{4\sqrt{2}}\hat{c}_{j+1,2k-1},\\
\hat{d}^-_{j,k} &:= \frac{2\sqrt{2}-1}{4\sqrt{2}}\hat{c}_{j+1,2k-1} - \frac{1}{2\sqrt{2}}\hat{c}_{j+1,2k} - \frac{1}{4\sqrt{2}}\hat{c}_{j+1,2k}.
\end{aligned}$$

The triplet $(d^0_{j,k}, d^+_{j,k}, d^-_{j,k})$ plays the role of the wavelet coefficient and it is jointly thresholded in order to preserve the density mass.

In the sequel of the paper, we shall denote W0 for the first algorithm based on the lifting scheme we have described and W1 for the second algorithm based on the quasi-interpolation operator. In the numerical scheme, we apply these algorithms and reconstruct the denoised density at the finest level J_0 on which we apply the Poisson solver to derive the electric field.

3 Numerical schemes

We present here the new scheme we introduce in the paper (PICONU[1]) as a modification of the classical PIC method which will be used to compare the numerical results. Of course, the considered Vlasov–Poisson equation is one dimensional in space and in velocity, so we can write a formal expression using the fundamental solution of the Poisson equation. Indeed, we have

$$-\triangle\Phi_{\text{self}} = \rho \iff \phi_{\text{self}} = \frac{-1}{2}|x| \iff E_{\text{self}} = \frac{1}{2}\frac{x}{|x|} * \rho.$$

On the other hand, if we denote $X_i(t)$ the position of the i^{th} particle at time t for $i = 1 \ldots N$, the density is

$$\rho(x,t) = \frac{1}{N}\Big(\sum_{i=1}^{N} \delta_{X_i(t)}\Big),$$

[1] which stands in French for PIC Ondelettes NUmérique

where δ_ξ stands for the Dirac measure at point ξ. Hence, the self-consistent field E_{self} can be computed by the following formula (written in general dimension d)

$$E_{\text{self}}(x,t) = \frac{1}{2N}\Big(\sum_{i=1}^{N} \frac{x - X_i}{|x - X_i|^d}\Big).$$

However, we underline that, in the practical point of view, we can not proceed in such a way in higher dimensions ($d > 1$) due to the singularity of the Green kernel, and that the adaptive method proposed in this paper is aimed at being extended, e.g., to the 2-D Vlasov–Poisson problem.

3.1 The PIC method

The PIC method consists in following the track to particles with position X_i and velocity V_i along the characteristic curves

$$\begin{aligned}
&\frac{dX_i(t)}{dt} = V_i(t),\\
&\frac{dV_i(t)}{dt} = E(X_i(t),t),\\
&X_i(0) = x_i,\ V_i(0) = v_i.
\end{aligned}$$

Let f_0 be the initial distribution, the distribution at time $t = T$ is computed as follows:

- Initialization: build (x_i, v_i), N pair of random variables drawn of the initial distribution f_0.

- Time marching scheme: the (nonlinear) characteristic equation is split and integrated as follows: set $\delta t = \frac{T}{N_{\max}}$ where $N_{\max}$ is the number of time steps, then, for $n = 0, \ldots, N_{\max}$

$$V^{n+1/2} = V^n + \frac{\delta t}{2} E^n(X^n) \tag{3.1a}$$

$$X^{n+1} = X^n + \delta t\, V^{n+1/2} \tag{3.1b}$$

$$\texttt{Build } \rho^{n+1} \tag{3.1c}$$

$$\texttt{Solve } -\Delta_h \phi^{n+1} = \rho^{n+1} \tag{3.1d}$$

$$E^{n+1}(X^{n+1}) = \nabla_h \phi^{n+1}(X^{n+1}) \tag{3.1e}$$

$$V^{n+1} = V^{n+1/2} + \frac{\delta t}{2} E^{n+1}(X^{n+1}) \tag{3.1f}$$

- Build $f^{N_{\max}}$ by interpolation.

In step 3.1c, we must compute the charge density ρ on the discrete grid points. Two classical methods are Nearest Grid Point (NGP) and Cloud In Cell (CIC): they consist on $P0$ and $P1$ interpolations respectively. According to Birdsall and Langdon in [3, p. 19–23], CIC reduces the noise relative to the NGP. Higher order techniques could be used too, some of them consist on quadratic and cubic spline interpolations. In our numerical results, we will compare our schemes to a PIC method with CIC and NGP density reconstruction.

3.2 The adaptive scheme (PICONU)

The PICONU scheme differs from the classical PIC method in the step (3.1c). The density is computed by Donoho's technique described in Section 2. For this method, we have to select the finest and the coarsest resolution level (J_0 and J_1), the threshold and the mesh size for the Poisson equation (3.1d). In the classical density estimation, the noise appears when the mesh size is locally too small. We expect to find the "good threshold" which refines the density mesh only in the region where there are a lot of particles.

4 Numerical results

The numerical results presented hereafter were obtained with SCILAB, the (free) numerical software of the INRIA [13]. As a validation of our scheme, we consider the simulation of the so-called Landau damping. This is indeed a significant numerical test, due to its difficulty in simulating, and it has been considered by several authors for validating a code, see, e.g., [3], [9] and references therein. This test consists in the observation of the decay rate of the electrostatic energy obtained when the initial distribution is the perturbed Maxwellian distribution defined by

$$f_0(x, v) = \frac{1}{\sqrt{2\pi}} \exp\left(-v^2/2{v_{\text{th}}}^2\right)(1 + \alpha \cos(kx)) \quad \text{for all } (x, v) \in \left[-\frac{L}{2}, \frac{L}{2}\right] \times \mathbb{R},$$

where v_{th} is the thermal mean velocity, $L = \frac{2\pi}{k}$ and k, α are positive constants with $\alpha \ll 1$. Let us recall that if E denotes the electric field, the electrostatic energy is defined by $\int_{-L/2}^{L/2} E^2\, dx$. We consider that the tail of the distribution does not contribute to the problem for $|v| > v_{\max}$ for some $v_{\max}$ large enough. We will choose $v_{\text{th}} = 1$ and $v_{\max} = 6$.

More precisely, one must observe numerically that

- The decay rate of electrostatic energy defines a line of director coefficient

$$\gamma_L = \sqrt{\frac{\pi}{8}} k^{-3} \exp\left(-\frac{1}{2k^2} - \frac{3}{2}\right),$$

- Oscillations frequency of the electrostatic energy must be

$$\omega^2 = 1 + 3k^2.$$

The Landau damping is very sensitive to the initial distribution and we follow [3] using for that purpose the so-called "quiet start" initialization for α small enough. For all the tests, we do vary only α taking as fixed value $k = 0.5$.

4.1 Comparison between NGP and W0

As a reference for validating our new scheme, we shall compare the results obtained with the classical PIC method where the charge density is computed using the NGP technique described in [3, pp. 21, 22] to the wavelets build from Haar system. In the finest resolution level J_0 is equal to the coarsest one J_1, these two methods are equivalent. In Figures 1, 2 and 3 we plotted the charge density, the electrostatic field and the discrete electrostatic energy of the plasma. The graph of the electrostatic energy is in a log-scale and the line corresponds to the theoretical decay of director coefficient γ_L.

We used the following parameters: the time step δt is chosen equal to 0.1. The threshold is the one given in (2.6) and more precisely, we choose $\eta = 0.5 \times \sqrt{j/N}$. The finest and coarsest resolution levels are 6 and 2, this corresponds to about 800 particles per cell. Then we use NGP on a grid of 2^6 intervals.

The NGP method requires a high number of particles per cell. The only way to reduce it is to increase the accuracy of the interpolation. The wavelets, based on the same interpolation, inherit the same problem. However, we observe that wavelets allow to reduce efficiently the noise of the method. This is obvious in Figure 3 and 4 looking at the minima of electrostatic energy: the local minima are obtained theoretically when the electrostatic field vanishes and numerically, these minima have the same magnitude than the discrete L^2-norm of the noise. Furthermore, we observe that the charge density and the electrostatic field are smoother than in the simple $P0$ interpolation case. Whatever noisy is the charge density, the electrostatic field is nearly smooth. It is due to the particular case of the one dimensional integration which has a smoothing effect. In higher dimension, the smoothness will take a greater importance and the use of wavelets should be more pertinent.

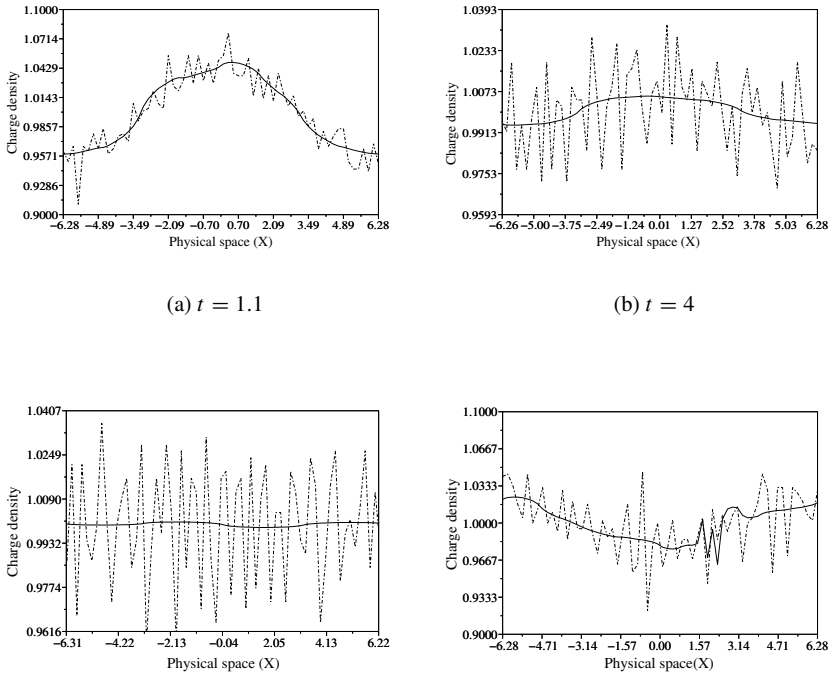

(a) $t = 1.1$ (b) $t = 4$

(c) $t = 6.1$ (d) $t = 7.4$

Figure 1. Landau damping with $\alpha = 0.1$. Charge density computed with 26000 particles, in solid line: the PICONU method (W0), in dashed line: the classical PIC (NGP).

4.2 Comparison between CIC and W1

The simulation parameters are chosen as follows: the highest level of resolution equals 7 and the number of particles equals 10 000. It implies that there is about 80 particles per cell. The time step δt equals 0.1. For the density estimation using wavelets, the coarsest resolution level is equal to 3 and the threshold is this one prescribed by Donoho, that is $K \times \sqrt{j/N}$. The coefficient R_T gives the rate of thresholded coefficients that is the ratio of the mean value of thresholded coefficients at each time step. Figure 5 gives the electrostatic energy computed with the classical PIC (CIC). We observe that the classical PIC fails when α becomes small. On the contrary, the adaptive method gives some better results (see Figure 6). A finer analysis of the threshold shows that all the coefficients are thresholded on the two finest grid. This is a natural consequence of the landau test: the distribution of particles corresponds to a small perturbation of the uniform distribution. Since we use only a first order reconstruction, the charge density is less smooth than in the case of W0.

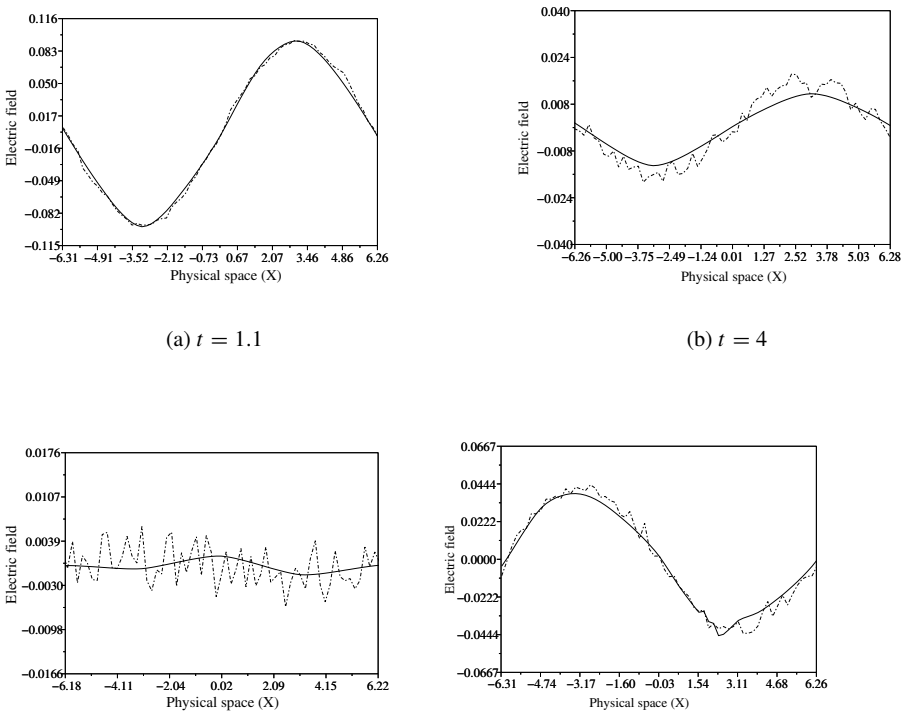

(a) $t = 1.1$ (b) $t = 4$

(c) $t = 6.1$ (d) $t = 7.4$

Figure 2. Landau damping with $\alpha = 0.1$. Electrostatic field computed with 26 000 particles, in solid line: the PICONU method (W0), in dashed line: the classical PIC (NGP).

5 Concluding remarks and perspectives

The results presented in this paper show that the adaptive wavelet reconstruction of the density for the Vlasov–Poisson equation is a promising approach to solve such plasma dynamics in a Lagrangian framework even though the choice of appropriated wavelets must still be discussed. The W0 wavelets are not completely satisfying because they require a high number of particles. Moreover, these methods are unable to verify the landau damping test for small perturbation magnitude α. We are interested in the numerical simulation where there are less than 100 particles per cell. The W1 wavelets satisfy this condition but do not smooth the density. The results proved that threshold helps to find the appropriate (adaptive) mesh and it should become crucial in tests where particles are very dispersed. Moreover, highest order reconstruction is

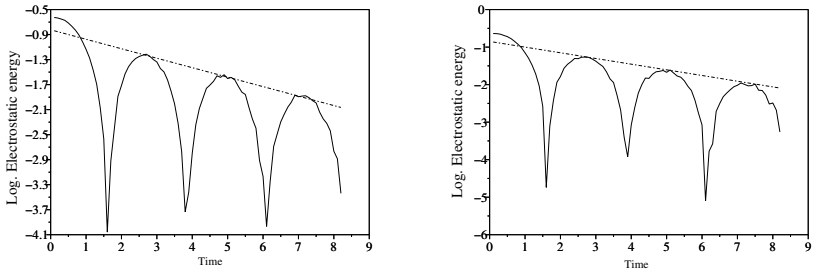

(a) Classical PIC (NGP) (b) PICONU method (W0)

Figure 3. Landau damping with $\alpha = 0.1$, $k = 0.5$. Electrostatic energy.

particularly efficient to reduce the noise. A compromise has to be found between the reconstruction and accuracy order which minimize the computational time.

We have considered here one dimensional Vlasov–Poisson but our approach will be extended in the near future to higher dimensional problems for which the Eulerian framework becomes more costly in terms of CPU time since large numbers of grid points must be used in that case.

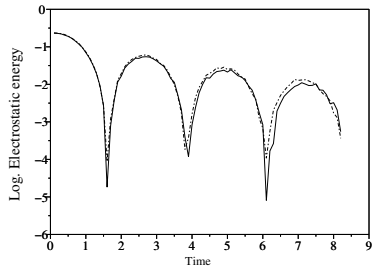

Figure 4. Superposition of electrostatic energy with 26 000 particles. In solid line: damping obtained with PICONU method (W0); in dashed line: classical PIC method (NGP).

Acknowledgements. The authors are very grateful to Prof. Eric Sonnendrücker for the numerous discussions we had with him and for the precious advice he gave us.

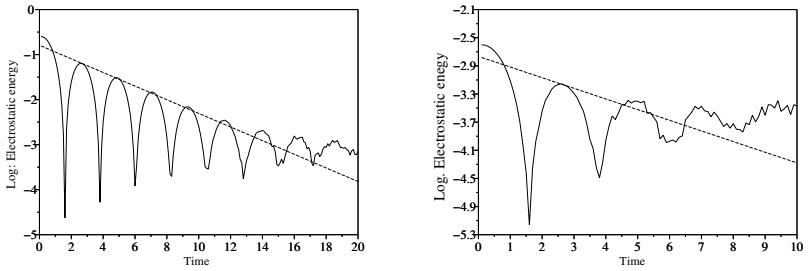

(a) $\alpha = 0.1$ (b) $\alpha = 0.01$

Figure 5. Linear Landau damping with classical PIC (CIC). 10 000 particles, 128 cells.

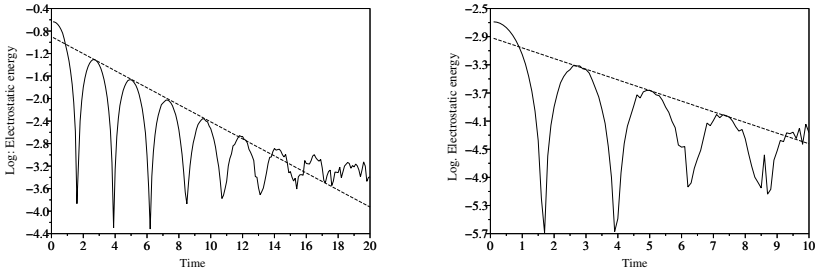

(a) $\alpha = 0.1,\ R_T = 13\%,\ K = 0.5$ (b) $\alpha = 0.01,\ R_T = 96\%,\ K = 1.5$

Figure 6. Linear Landau damping, PICONU (W1), 10 000 particles.

References

[1] Arber, T. D., Vann, R. G. L., A critical comparison of Eulerian-Grid-Based Vlasov solvers, *J. Comput. Phys.* 180 (2002), 339–357.

[2] Besse, N., Sonnendrücker, E., Semi-Lagrangian schemes for the Vlasov equation on an unstructured mesh of phase space. J. Comput. Phys. 191 (2) (2003), 341–376.

[3] Birdsall, C. K., Langdon, A. B., *Plasma Physics via Computer Simulation*, Institute of Physics Publishing, Bristol and Philadelphia 1991.

[4] Chapman, S., Cowling, T. G., *The mathematical theory of non-uniform gases*, An account of the kinetic theory of viscosity, thermal conduction and diffusion in gases, third edition, prepared in co-operation with D. Burnett, Cambridge University Press, London 1970. Chapman, S. Cowling, T. G. The mathematical theory of non-uniform gases.

[5] Cohen, A., *Numerical Analysis of Wavelet Methods*, Stud. Math. Appl. 32, Elsevier, North-Holland, Amsterdam 2003.

[6] Cottet, G.-H., Raviart, P.-A., Particle methods for the one-dimensional Vlasov-Poisson equations, *Siam J. Numer. Anal.* 21 (1) (1984), 52–76.

[7] Daubechies, I., *Ten Lectures on Wavelets*, CBMS-NSF Reg. Conf. Ser. Appl. Math. 61, SIAM, Philadelphia, PA, 1992.

[8] Donoho D. L., Johnstone I. M., Kerkyacharian G., Picard, D., Density estimation by wavelet thresholding, *Ann. Statist.* 24 (2) (1996), 508–539.

[9] Filbet, F., Contribution à l'analyse et la simulation numérique de l'équation de Vlasov, Thèse, Université Henri Poincaré, Nancy, France, 2001.

[10] Filbet, F., Sonnendrücker, E., Bertrand, P., Conservative numerical schemes for the Vlasov equation, *J. Comput. Phys.* 172 (2001), 166–187.

[11] Harten, A., Discrete multi-resolution analysis and generalized wavelets, *Appl. Numer. Math.* 12 (1993), 153–193.

[12] Raviart, P. A., An analysis of particle methods, in *Numerical methods in fluid dynamics*, Lecture Notes in Math. 1127, Springer-Verlag, Berlin 1985, 243–324.

[13] Scilab, `http://scilabsoft.inria.fr`

[14] Sweldens, W., The lifting scheme: a custom design construction of biorthogonal wavelets, *Appl. Comput. Harmon. Anal.* 3 (1996), 186–200.